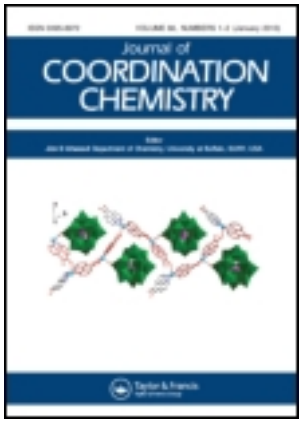

Journal of Coordination Chemistry
Publication details, including instructions for authors and subscription information:
http://www.tandfonline.com/loi/gcoo20

A Schiff base bis(N-salicylidene)-3-oxapentane-1,5-diamine and its yttrium(III) complex: synthesis, crystal structure, DNA-binding properties, and antioxidant activities

Huilu Wu [a], Guolong Pan [a], Yuchen Bai [a], Hua Wang [a], Jin Kong [a], Furong Shi [a], Yanhui Zhang [a] & Xiaoli Wang [a]
[a] School of Chemical and Biological Engineering, Lanzhou Jiaotong University, Lanzhou, P.R. China

Accepted author version posted online: 11 Jun 2013.Published online: 16 Jul 2013.

To cite this article: Huilu Wu, Guolong Pan, Yuchen Bai, Hua Wang, Jin Kong, Furong Shi, Yanhui Zhang & Xiaoli Wang (2013) A Schiff base bis(N-salicylidene)-3-oxapentane-1,5-diamine and its yttrium(III) complex: synthesis, crystal structure, DNA-binding properties, and antioxidant activities, Journal of Coordination Chemistry, 66:15, 2634-2646, DOI: 10.1080/00958972.2013.812725

To link to this article: http://dx.doi.org/10.1080/00958972.2013.812725

Journal of Coordination Chemistry, 2013
Vol. 66, No. 15, 2634–2646, http://dx.doi.org/10.1080/00958972.2013.812725

A Schiff base bis(*N*-salicylidene)-3-oxapentane-1,5-diamine and its yttrium(III) complex: synthesis, crystal structure, DNA-binding properties, and antioxidant activities

HUILU WU*, GUOLONG PAN, YUCHEN BAI, HUA WANG, JIN KONG, FURONG SHI, YANHUI ZHANG and XIAOLI WANG

School of Chemical and Biological Engineering, Lanzhou Jiaotong University, Lanzhou, P.R. China

(*Received 5 January 2013; in final form 18 April 2013*)

A Schiff base bis(*N*-salicylidene)-3-oxapentane-1,5-diamine (H_2L) and its yttrium(III) (Y(III)) complex, $Y_2L_2(NO_3)_2{\cdot}2H_2O$, have been synthesized and characterized by physico-chemical and spectroscopic methods. The crystal structure of the Y(III) complex has been determined by single-crystal X-ray diffraction, revealing a centrosymmetric binuclear neutral entity where Y(III) centers are bridged by two phenoxo oxygens. The DNA-binding properties of the Schiff base H_2L and the Y(III) complex were investigated by spectrophotometric methods and viscosity measurements. The results suggest that ligand H_2L and Y(III) complex both bind to DNA *via* groove binding, and the Y(III) complex binds to DNA more strongly than H_2L. The antioxidant activity of the Y(III) complex was determined by superoxide and hydroxyl radical-scavenging method *in vitro*, which indicates that Y(III) complex scavenges $OH\cdot$ and $O_2^{-\cdot}$ radicals.

Keywords: Bis(*N*-salicylidene)-3-oxapentane-1, 5-diamine; Yttrium(III) complex; Crystal structure; DNA-binding property; Antioxidant activities

1. Introduction

Binding of small molecules with DNA has been studied extensively since DNA is the material of inheritance and controls the structure and function of cells [1]. Small molecules possessing DNA-binding abilities include metal complexes, porphyrins, natural antibiotics, simple aromatic hydrocarbons, and some heterocyclic cations [2–7]. Particularly, the DNA binding of metal complexes is studied for probes of nucleic acid structure, DNA footprinting, and sequence-specific cleaving agents, antitumor drugs, etc. [8–10]. An understanding of how these small molecules bind to DNA will be useful in the design of new compounds, which can recognize specific sites or conformations of DNA [11–13].

Schiff base complexes have been among the most widely studied coordination compounds, increasingly important as biochemical, analytical, and antimicrobial reagents [14]. Biological activity and other applications result in increasing interest for lanthanides [15–19]. One of the most studied applications is the use of lanthanide complexes to address DNA/RNA by non-covalent binding and/or cleavage [20–23].

*Corresponding author. Email: wuhuilu@163.com

Lanthanide ions are oxophilic and we select the yttrium(III) (Y(III)) complex with a pentadentate Schiff base bis(*N*-salicylidene)-3-oxapentane-1,5-diamine. The DNA-binding properties of the complex were investigated by spectrophotometric and viscosity measurements. In addition, the antioxidant activities of the complex were determined by superoxide anion (O_2^-) and hydroxyl radical (OH·)-scavenging methods *in vitro*.

2. Experimental

2.1. *Materials and methods*

All chemicals were of analytical grade. Calf thymus DNA (CT-DNA), ethidium bromide (EB), nitroblue tetrazolium nitrate (NBT), methionine (MET), and riboflavin ($VitB_2$) were obtained from Sigma-Aldrich Co. (USA) and used without purification. All experiments involving interaction of the ligand and the complex with CT-DNA were carried out in doubly-distilled water buffer containing 5 mM Tris and 50 mM NaCl adjusted to pH 7.2 with hydrochloric acid. A solution of CT-DNA gave a ratio of UV absorbance at 260 and 280 nm of about 1.8–1.9, indicating that the CT-DNA was sufficiently free of protein [24]. The CT-DNA concentration per nucleotide was determined spectrophotometrically by employing an extinction coefficient of 6600 L/M cm at 260 nm [25].

C, H, and N elemental analyses were determined using a Carlo Erba 1106 elemental analyzer. IR spectra were recorded from 4000 to 400 cm^{-1} with a Nicolet FT-VERTEX 70 spectrometer using KBr pellets. Electronic spectra were taken on Lab-Tech UV Bluestar and Spectrumlab 722sp spectrophotometers with a spectral resolution of 0.2 nm. Fluorescence spectra were recorded on a LS-45 spectrofluorophotometer. ^1H NMR spectra were obtained with a Mercury plus 400 MHz NMR spectrometer with TMS as an internal standard and $CDCl_3$ as the solvent.

The synthetic route for H_2L is shown in scheme 1.

2.2. *Preparation of H_2L and its complex*

2.2.1. Preparation of 3-oxapentane-1,5-diamine. 3-Oxapentane-1,5-diamine was synthesized following the procedure [26]. 1,5-Dichloro-3-oxapentane was prepared by the reaction of diethylene glycol and thionyl chloride. Dichloride, potassium phthalimide, and diethylamine were heated together at 140 °C for 3 h to synthesize 3-oxapentane-1,5-diphthalimide. After a series of hydrolysis, acidification, and distillation, a colorless oil was obtained. Anal. Calcd (%) for $C_4H_{12}N_2O$: C, 46.25; H, 11.54; N, 26.90.

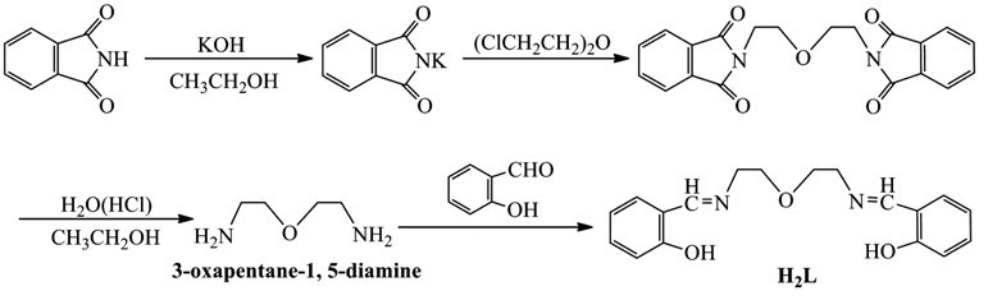

Scheme 1. Synthetic routine of H_2L.

Found (%): C, 45.98; H, 11.50; N, 26.76. FT–IR (KBr ν/cm^{-1}): 1120 ν(C–O–C), 3340 ν(–NH_2) stretching frequency, respectively.

2.2.2. Bis(N-salicylidene)-3-oxapentane-1,5-diamine (H_2L). For the synthesis of H_2L, salicylic aldehyde (10 mM, 1.22 g) in EtOH (5 mL) was added dropwise to 5 mL of an EtOH solution of 3-oxapentane-1,5-diamine (5 mM, 0.52 g). After completion of addition, the solution was stirred for an additional 4 h at 78 °C. After cooling to room temperature, the precipitate was filtered. The product was dried in vacuo, giving a yellow crystalline solid. Yield: 1.19 g (68.5%). Anal. Calcd (%) for $C_{18}H_{20}O_3N_2$: C, 69.21; H, 6.45; N, 8.97. Found (%): C, 69.09; H, 6.54; N, 8.83. ^{1}H-NMR ($CDCl_3$ 400 MHz) δ/ppm: 8.30 (s, 2H, N = C–H), 6.79–7.33 (m, 8H, H-benzene ring), 3.66–3.74 (m, 8H, O–$(CH_2)_2$–N = C). UV-vis (λ, nm): 268, 316. FT–IR (KBr ν/cm^{-1}): 1637 ν(C = N), 1286 ν(C–O–C), 3458 ν(OH), stretching frequency, respectively.

2.2.3. Synthesis of $Y_2L_2(NO_3)_2{\cdot}2H_2O$. To a stirred solution of H_2L (0.156 g, 0.5 mM) in EtOH (10 mL) were added $Y(NO_3)_3(H_2O)_6$ (0.191 g, 0.5 mM) and triethylamine (0.3 mL) in EtOH (10 mL). A yellow sediment was generated rapidly. The precipitate was filtered off, washed with EtOH and absolute Et_2O, and dried in *vacuo*. The dried precipitate was dissolved in DMF to form a yellow solution. Yellow block crystals of $Y_2L_2(NO_3)_2{\cdot}2H_2O$ suitable for X-ray diffraction studies were obtained by vapor diffusion of diethyl ether into the solution for a few weeks at room temperature. Yield: 0.198 g (57.1%). Anal. Calcd (%) for $C_{36}H_{40}Y_2N_6O_{14}$: C, 45.10; H, 4.18; N, 8.77. Found (%): C, 44.99; H, 4.26; N, 8.63. UV-vis (λ, nm): 269, 316. FT–IR (KBr ν/cm^{-1}): 1230 ν(C–O–C), 1378 $\nu_s(NO_3)$, 1052 $\nu_a(NO_3)$, 1631 ν(C = N) stretching frequency, respectively.

2.3. *X-ray crystallography*

A suitable single crystal was mounted on a glass fiber and intensity data were collected on a Bruker Smart CCD diffractometer with graphite-monochromated Mo-Kα radiation (λ = 0.71073 Å) at 296 K. Data reduction and cell refinement were performed using SMART and SAINT programs [27]. The structure was solved by direct methods and refined by full-matrix least-squares against F^2 of data using SHELXTL [28]. All hydrogens were found in difference electron maps and subsequently refined in a riding-model approximation with C–H distances ranging from 0.93–0.97 Å and U_{iso} (H) = 1.2 U_{eq} (C) or 1.5 U_{eq} (C).

2.4. *DNA-binding experiments*

2.4.1. Viscosity titration measurements. Viscosity experiments were conducted on an Ubbelodhe viscometer, immersed in a water bath maintained at 25.0 ± 0.1 °C. Titrations were performed for the complexes (3–30 μM) and each compound was introduced into the CT-DNA solution (42.5 μM) present in the viscometer. Data were analyzed as $(\eta/\eta_0)^{1/3}$ *versus* the ratio of the concentration of the compound to CT-DNA, where η is the viscosity of CT-DNA in the presence of the compound and η_0 is the viscosity of CT-DNA alone. Viscosity values were calculated from the observed flow time of CT-DNA-containing solutions corrected from the flow time of buffer alone (t_0), $\eta = (t - t_0)$ [29].

2.4.2. Electronic absorption titration. Absorption titration experiments were performed with fixed concentrations of the complexes, while gradually increasing the concentration of CT-DNA. To obtain the absorption spectra, the required amount of CT-DNA was added to both the compound and reference solutions, in order to eliminate the absorbance of CT-DNA itself. From the absorption titration data, the binding constant (K_b) was determined using the equation [30]:

$$[\mathrm{DNA}]/(\varepsilon_a - \varepsilon_f) = [\mathrm{DNA}]/(\varepsilon_b - \varepsilon_f) + 1/K_b(\varepsilon_b - \varepsilon_f)$$

where [DNA] is the concentration of CT-DNA in base pairs, ε_a corresponds to the observed extinction coefficient (Aobsd/[M]), ε_f corresponds to the extinction coefficient of the free compound, ε_b is the extinction coefficient of the compound when fully bound to CT-DNA, and K_b is the intrinsic binding constant. The ratio of slope to intercept in the plot of $[\mathrm{DNA}]/(\varepsilon_a - \varepsilon_f)$ *versus* [DNA] gave the value of K_b.

2.4.3. Fluorescence studies. Enhanced fluorescence of EB in the presence of DNA can be quenched by the addition of a second molecule [31, 32]. The extent of fluorescence quenching of EB bound to CT-DNA can be used to determine the extent of binding between the second molecule and CT-DNA. Competitive binding experiments were carried out in the buffer by keeping [DNA]/[EB] = 1 and varying the concentrations of the compounds. The fluorescence spectra of EB were measured using an excitation wavelength of 520 nm and the emission range was set between 550 and 750 nm. The spectra were analyzed according to the classical Stern–Volmer equation [33]:

$$I_0/I = 1 + K_{SV}[Q]$$

where I_0 and I are the fluorescence intensities at 599 nm in the absence and presence of the quencher, respectively, K_{SV} is the linear Stern–Volmer quenching constant, and $[Q]$ is the concentration of the quencher. In these experiments, $[\text{CT-DNA}] = 2.5 \times 10^{-3}$ M/L, $[\mathrm{EB}] = 2.2 \times 10^{-3}$ M/L.

2.5. *Antioxidant property*

2.5.1. Hydroxyl radical assay. Hydroxyl radicals were generated in aqueous media through the Fenton-type reaction [34, 35]. Aliquots of the reaction mixture (3 mL) contained 1 mL of 0.1 mM aqueous safranin, 1 mL of 1.0 mM aqueous EDTA–Fe(II), 1 mL of 3% aqueous H_2O_2, and a series of quantitative microadditions of solutions of the test compound. A sample without the tested compound was used as the control. The reaction mixtures were incubated at 37 °C for 30 min in a water bath. Absorbance was then measured at 520 nm. All the tests were run in triplicate and are expressed as the mean and standard deviation (SD) [36]. The scavenging effect for OH· was calculated from the following expression:

$$\text{Scavenging ratio } (\%) = [(A_i - A_0)/(A_c - A_0)] \times 100\%$$

where A_i = absorbance in the presence of the test compound; A_0 = absorbance of the blank; A_c = absorbance in the absence of the test compound, EDTA-Fe(II) and H_2O_2.

2.5.2. Superoxide radical assay. A non-enzymatic system containing 1 mL 9.9×10^{-6} M VitB2, 1 mL 1.38×10^{-4} M NBT, and 1 mL 0.03 M MET was used to produce superoxide anion (O_2^-), and the scavenging rate of O_2^- under the influence of 0.1–1.0 μM of the tested compound was determined by monitoring the reduction in the rate of transformation of NBT to monoformazan dye [37]. The solutions of MET, VitB2, and NBT were prepared with 0.02 M phosphate buffer (pH = 7.8) in the absence of light. The reactions were monitored at 560 nm with a UV-vis spectrophotometer and the rate of absorption change was determined. The percentage inhibition of NBT reduction was calculated using the equation [38]: percentage inhibition of NBT reduction $= (1 - k'/k) \times 100$, where k' and k represent the slopes of the straight line of absorbance values as a function of time in the presence and absence of SOD mimic compound (SOD is superoxide dismutase), respectively. The IC_{50} values for the complexes were determined by plotting the graph of percentage inhibition of NBT reduction against the increase in the concentration of the complex. The concentration of the complex which causes 50% inhibition of NBT reduction is reported as IC_{50}.

3. Results and discussion

H_2L and Y(III) complex are stable in air. The Y(III) complex is remarkably soluble in polar aprotic solvents such as DMF, DMSO, and MeCN, slightly soluble in ethanol, methanol, ethyl acetate, and chloroform and insoluble in water, Et_2O, and, petroleum ether.

3.1. *IR and electronic spectra*

For free H_2L, a strong band is found at 1637 cm^{-1} with a weak band at 1286 cm^{-1}. By analogy with assigned bands, the former can be attributed to ν(C = N), while the latter can be attributed to ν(C–O–C). These bands shift to lower frequency by ca. 6–56 cm^{-1} for the Y(III) complex [39], which implies direct coordination of nitrogen and oxygen. The bands at 1378 and 1052 cm^{-1} indicate that nitrate is bidentate [40] and a weak band at 3675 cm^{-1} is allocated as $\nu(H_2O)$, in agreement with the result of X-ray diffraction.

The electronic spectra of H_2L and Y(III) complex were recorded in DMF solution at room temperature. The UV bands of H_2L (268 and 316 nm) are marginally shifted in the complex. Two absorptions are assigned to $\pi \rightarrow \pi^*$ (benzene) and $\pi \rightarrow \pi^*$ (C = N) transitions [41].

3.2. *X-ray structure of the complex*

Basic crystal data, description of the diffraction experiment, and details of the structure refinement are given in table 1. Selected bond distances and angles are presented in table 2.

3.2.1. The crystal structure of $Y_2L_2(NO_3)_2 \cdot 2H_2O$. The crystal structure of the Y(III) complex consists of discrete $Y_2L_2(NO_3)_2$ and two H_2O molecules. The prepared pentadentate ligand contains strong donors, phenoxo and imine nitrogen with excellent coordination ability through its N_2O_3 donor set. Single-crystal X-ray structure determination reveals that the complex has a centrosymmetric neutral homobinuclear entity. An ORTEP illustration of the complex (figure 1(a)) shows that two adjacent [Y(L)(NO_3)] moieties are coupled together *via* two phenolato bridges belonging to the two ligands. In the μ_2-diphenoxo bridged binuclear structure, both the Y(III) centers are eight-coordinate (figure 1(b)).

Table 1. Crystal data and structure refinement for $Y_2L_2(NO_3)_2{\cdot}2H_2O$.

Complex	$Y_2L_2(NO_3)_2{\cdot}2H_2O$
Molecular formula	$C_{36}H_{40}Y_2N_6O_{14}$
Molecular weight	958.56
Color	Yellow
Crystal size, mm^3	$0.25 \times 0.23 \times 0.20$
Crystal system	Monoclinic
Space group	*C2/c*
a, Å	29.310(7)
b, Å	11.726(3)
c, Å	15.169(4)
α, deg	90
β, deg	118.039(2)
γ, deg	90
V, $Å^3$	4601.7(19)
Z	4
T, K	296(2)
D_{Calcd}, $g\,cm^{-3}$	1.384
F (000), e	1952
θ range for data collection, deg	2.20–25.50
hkl range	$-34 \leqslant h \leqslant 35,\ -14 \leqslant k \leqslant 13,\ -18 \leqslant l \leqslant 18$
Reflections collected	16,378
Independent reflections	4265 [$R_{int} = 0.0403$]
Refinement method	Full-matrix least-squares on F^2
Data/restraints/parameters	4265/3/262
Final R_1/wR_2 indices [$I \geqslant 2\sigma(I)$]	0.0397/0.1264
R_1/wR_2 indices (all data)	0.0706/0.1416
Goodness-of-fit on F^2	1.074
Largest diff. peak and hole, e $Å^{-3}$	0.743 and −0.274

Table 2. Selected bond distances (Å) and angles (°) in $Y_2L_2(NO_3)_2{\cdot}2H_2O$.

Complex	$Y_2L_2(NO_3)_2{\cdot}2H_2O$			
Bond distances	Y(1)–O(3)	2.164(3)	Y(1)–O(1)	2.451(3)
	Y(1)–O(2)#1[a]	2.271(3)	Y(1)–O(5)	2.470(3)
	Y(1)–O(2)	2.310(3)	Y(1)–N(2)	2.473(4)
	Y(1)–O(4)	2.450(3)	Y(1)–N(1)	2.505(4)
Bond angles	O(3)–Y(1)–O(2)#1	96.20(11)	O(3)–Y(1)–O(4)	96.20(13)
	O(3)–Y(1)–O(2)	85.94(10)	O(2)#1–Y(1)–O(4)	156.87(10)
	O(2)#1–Y(1)–O(2)	71.26(10)	O(2)–Y(1)–O(4)	129.11(10)
	O(2)–Y(1)–O(1)	131.42(10)	O(4)–Y(1)–O(1)	71.09(11)
	O(3)–Y(1)–O(1)	140.61(11)	O(3)–Y(1)–O(5)	83.01(12)
	O(2)#1–Y(1)–O(1)	87.02(10)	O(2)–Y(1)–O(5)	78.82(10)
	O(2)#1–Y(1)–O(5)	150.03(10)	O(4)–Y(1)–O(5)	51.34(10)
	O(1)–Y(1)–O(5)	112.52(11)	O(3)–Y(1)–N(2)	74.72(13)
	O(2)#1–Y(1)–N(2)	84.90(11)	O(2)–Y(1)–N(2)	147.48(12)
	O(1)–Y(1)–N(2)	66.46(13)	O(4)–Y(1)–N(2)	79.65(12)
	O(3)–Y(1)–N(1)	152.38(12)	O(5)–Y(1)–N(2)	123.14(11)
	O(2)–Y(1)–N(1)	70.64(11)	O(2)#1–Y(1)–N(1)	90.07(11)
	O(4)–Y(1)–N(1)	87.93(13)	O(1)–Y(1)–N(1)	66.38(11)
	O(5)–Y(1)–N(1)	78.36(11)	N(2)–Y(1)–N(1)	132.76(13)

[a]Symmetry transformations used to generate equivalent atoms: #1 $-x+1/2, -y+3/2, -z$.

The local coordination environment is identical for both centers and is best described as a distorted square YN_2O_6 antiprism (figure 1(c)). Due to flexibility of the ligand, it loses planarity. The bond distances are Y(1)–N_{imine}: 2.473(4)–2.505(4), Y(1)–O_{ether}: 2.451(3), and Y(1)–$O_{nitrate}$: 2.450(3)–2.470(3) Å. Coordination of the two identical Schiff bases of the

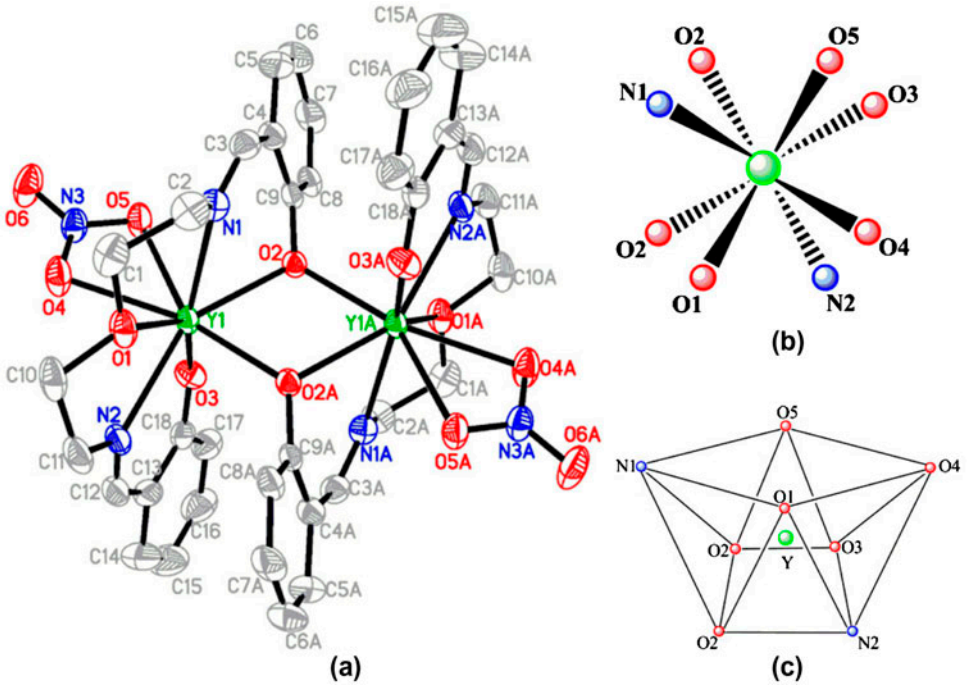

Figure 1. (a) The molecular structure of $Y_2L_2(NO_3)_2$ in the crystal with displacement ellipsoids at 30% probability level; hydrogens are omitted for clarity, (b) perspective disposition of the donor sites around each Y^{3+} center shown in Neumann projection, (c) a distorted square antiprism geometry is formed by donors around Y^{3+} as illustrated in the polyhedral view.

same ligand is different. Of the two phenoxo oxygens of each ligand, one is simply monocoordinated while the other bridges the adjacent Y(III) centers as reflected by the $Y–O_{phenoxo}$ bond lengths [Y(1)–O(2), 2.310(3) and Y(1)–O(3), 2.146(3) Å]. The distance of Y(1)–Y(1A), 3.7230(11) Å, is relatively too long to consider any direct Y–Y interaction.

Hydrogen-bonding interactions play important roles in crystal packing in the complex [42]. The hydrogen C(11) forms a hydrogen bond to O(6) with dimensions C···O 3.46 Å, C–H···O 145.4°, and H···O 2.62 Å to result in a 1-D polymeric structure (figure 2). An

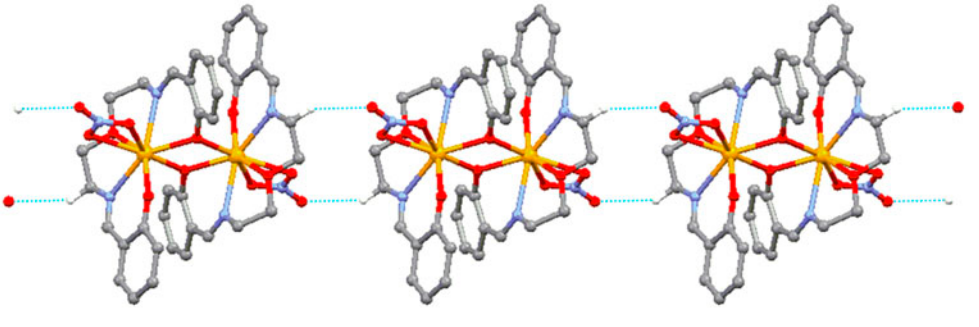

Figure 2. Packing diagram of Y(III) complex showing the 1D H-bonded network; hydrogens except H(11B) have been excluded for clarity.

interesting feature of this structure is the intermolecular hydrogen bond that exists among the Y(III) complexes, which also affords voids to trap guest molecules, suggesting potential application for gas absorption [43].

3.3. *DNA-binding properties*

3.3.1. Viscosity titration measurements. Viscosity titration measurements were carried out to further clarify the interaction between the investigated compounds and CT-DNA. Hydrodynamic measurements that are sensitive to changes in the length of DNA (i.e. viscosity and sedimentation) are critical tests of binding in solution in the absence of crystallographic structural data [44]. The classic intercalation model involves insertion of a planar molecule between DNA base pairs, which results in a decrease in the DNA helical twist and lengthening of the DNA; the molecule will be in close proximity to the DNA base pairs as well [45–47]. In contrast, the molecule that binds exclusively in the DNA grooves by partial and/or non-classical intercalation, under the same conditions, typically causes less pronounced (positive or negative) or no change in the DNA solution viscosity [48, 49].

The effects of H_2L and Y(III) complex on the viscosity of CT-DNA are shown in figure 3. The experimental results indicate that the addition of H_2L and Y(III) complex causes no significant viscosity change. Therefore, according to the previous report related to DNA-binding lanthanide complexes [50–54], we can deduce that H_2L and Y(III) complex probably bind to DNA in a groove mode.

3.3.2. Absorption spectroscopic studies. Application of electronic absorption spectroscopy in DNA-binding studies is one of the most useful techniques [55]. To clarify the interactions between the compounds and DNA, the electronic absorption spectra of H_2L and its Y(III) complex in the absence and presence of the CT-DNA (at a constant concentration of the compounds) were obtained, as shown in figure 4. With increasing DNA concentrations, the absorption bands at 394 nm of H_2L show a hypochromism of 32.35%; the absorption bands at 393 nm of the Y(III) complex show a hypochromism of 58.24%.

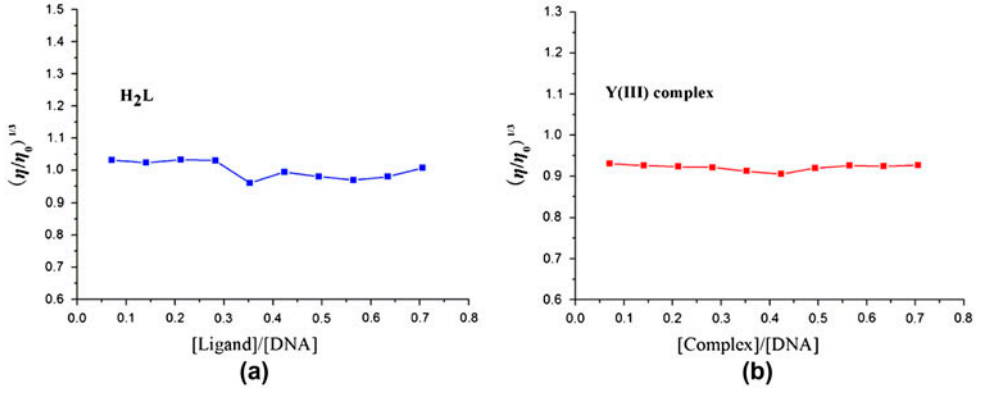

Figure 3. Effect of increasing amounts of (a) H_2L and (b) Y(III) complex on the relative viscosity of CT-DNA at 25.0 ± 0.1 °C.

Hypochromism observed for the $\pi \rightarrow \pi^*$ transitions indicate strong binding of H_2L and complex to DNA.

To compare quantitatively the affinity of H_2L and Y(III) complex towards DNA, the intrinsic binding constants K_b of the two compounds to CT-DNA were determined by monitoring the changes of absorbance with increasing concentrations of DNA. The intrinsic binding constant K_b of H_2L and of the Y(III) complex were $5.30 \times 10^3\,M^{-1}$ ($R = 0.99$ for 16 points) and $2.30 \times 10^4\,M^{-1}$ ($R = 0.99$ for 16 points), respectively, from the decay of the absorbances. The K_b values obtained here are lower than that reported for a classical intercalator (for EB and [Ru(phen)DPPZ], the binding constants are of the order of 10^6–$10^7\,M^{-1}$) [56–59]. It is clear that the hypochromism and K_b values are not enough evidence, but these results suggest an intimate association of the compounds with CT-DNA and indicate that the binding strength of the complex is higher than that for H_2L.

Based on the above results, the affinity for DNA is stronger for the Y(III) complex than the ligand. We attribute the reason as the charge transfer of coordinated H_2L caused by coordination which results in the decrease of charge density of the planar conjugated system. This change will lead to complexes binding to DNA more readily [60, 61]. The

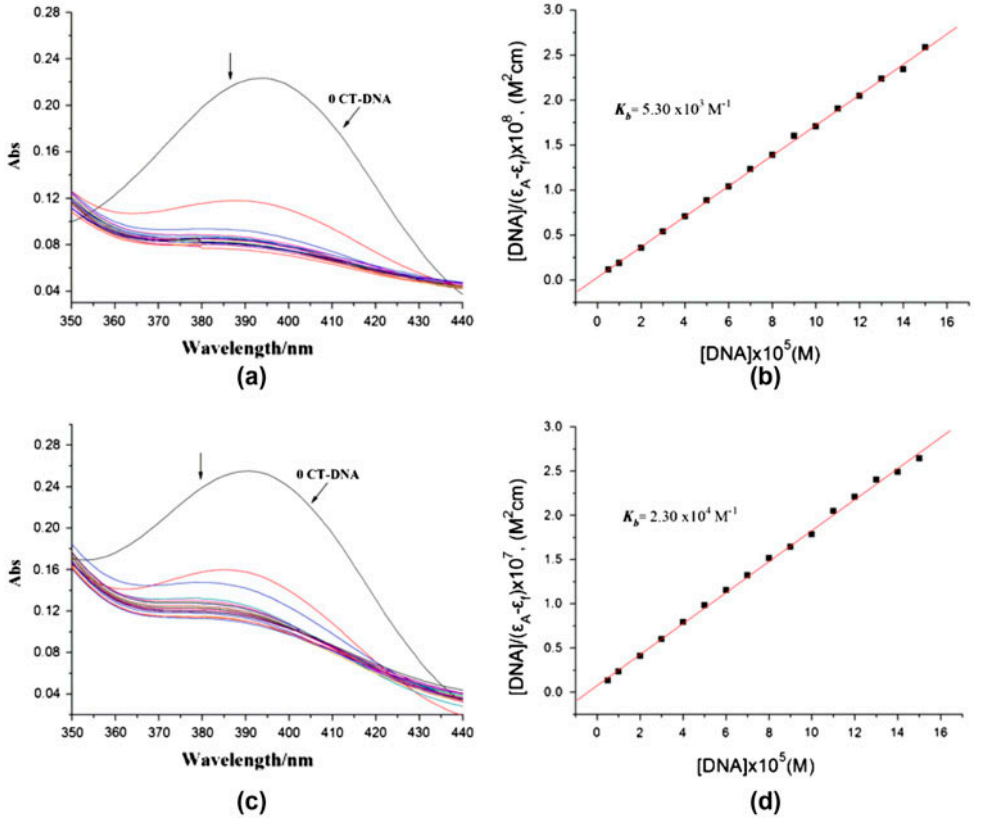

Figure 4. Electronic spectra of (a) H_2L, (c) Y(III) complex in Tris–HCl buffer upon the addition of CT-DNA. [Compound] = 3×10^{-5} M, [DNA] = 2.5×10^{-5} M. Arrow shows the emission intensity changes upon increasing DNA concentration. Plots of $[DNA]/(\varepsilon_a - \varepsilon_f)$ *vs.* [DNA] for the titration of (b) H_2L, (d) Y(III) complex with CT-DNA.

helical structure of the Y(III) complex is able to provide lots of groove positions to stack more strongly with the base pairs of the DNA helix [62].

3.3.3. Fluorescence spectroscopic studies. To further study the binding properties of the complexes with DNA, competitive binding was carried out. Relative binding of H_2L and Y(III) complex to CT-DNA was studied by the fluorescence spectral method using ethidium bromide (EB)-bound CT-DNA solution in the Tris-HCl/NaCl buffer (pH = 7.2). As a typical indicator of intercalation, EB is a weak fluorescent compound. But in the presence of DNA, the emission intensity of EB is greatly enhanced because of its strong intercalation between the adjacent DNA base pairs [32]. In general, measurement of the ability of a complex to affect the intensity of EB fluorescence in the EB-DNA adduct allows the determination of the affinity of the complex for DNA, whatever the binding mode may be. If a complex can displace EB from DNA, the fluorescence of the solution will be reduced due to free EB molecules that are readily quenched by water [63]. For H_2L and the Y(III) complex, no emission was observed either alone or in the presence of CT-DNA in the buffer. The fluorescence quenching of DNA–bound EB by the ligand and the complex are shown in figure 5. The behavior of H_2L and Y(III) complex is in agreement with the Stern–Volmer equation, which provides further evidence that the two compounds bind to DNA. The K_{sv} values for H_2L and Y(III) complex are 0.35×10^4 (R = 0.98 for 21 points) and $1.25 \times 10^4\,M^{-1}$ (R = 0.99 for 13 points), respectively, reflecting the higher quenching efficiency of the Y(III) complex relative to that of H_2L. This suggests that DNA-binding of the Y(III) complex is stronger than that of H_2L. Such a trend is consistent with the absorption spectral results.

3.4. *Antioxidant property*

According to relevant reports in the literature [64, 65], rare earth complexes may exhibit antioxidant activity. We, therefore, conducted an investigation to explore whether the Y(III) complex has antioxidant activities.

3.4.1. Hydroxyl radical-scavenging activity. We compared the abilities of the present compounds to scavenge hydroxyl radicals with those of the well-known natural antioxidants mannitol and vitamin C, using the same method as reported in a previous paper [66]. The 50% inhibitory concentrations (IC_{50}) of mannitol and vitamin C are 9.6×10^{-3} and $8.7 \times 10^{-3}\,M^{-1}$, respectively. As shown in figure 6(a), according to the antioxidant experiments, the IC_{50} value of Y(III) complex is $3.73 \times 10^{-5}\,M^{-1}$, which implies that the Y(III) complex exhibits better scavenging activity than mannitol and vitamin C. Much less scavenging activity was exhibited by H_2L when compared to that of Y(III) complex. Due to the observed IC_{50} values, the Y(III) complex can be considered as a potential drug to eliminate the hydroxyl radical.

3.4.2. Superoxide radical-scavenging activity. As another assay of antioxidant activity, superoxide radical (O_2^-)-scavenging activity has been investigated. The Y(III) complex has good superoxide radical-scavenging activity.

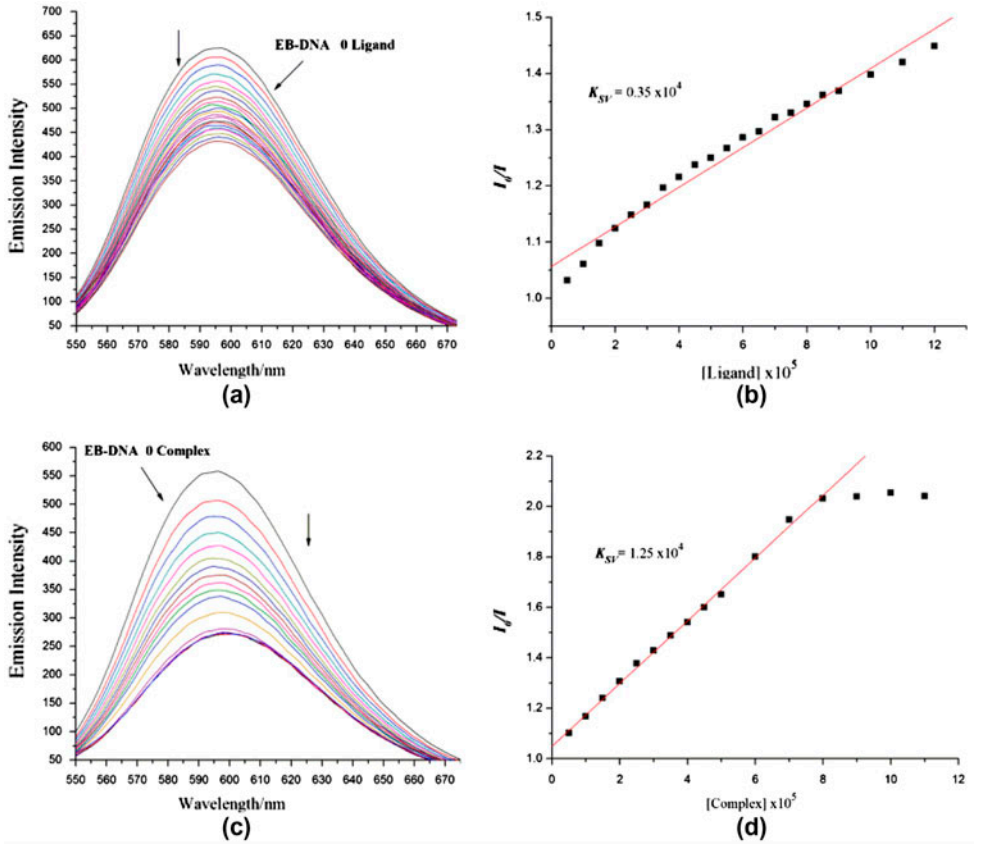

Figure 5. Emission spectra of EB bound to CT-DNA in the presence of (a) H_2L and (c) Y(III) complex; [compound] = 3×10^{-5} M; λ_{ex} = 520 nm. The arrows show the intensity changes upon increasing concentrations of the complexes. Fluorescence quenching curves of EB bound to CT-DNA by (b) H_2L and (d) Y(III) complex. (Plots of I_0/I *vs.* [complex].)

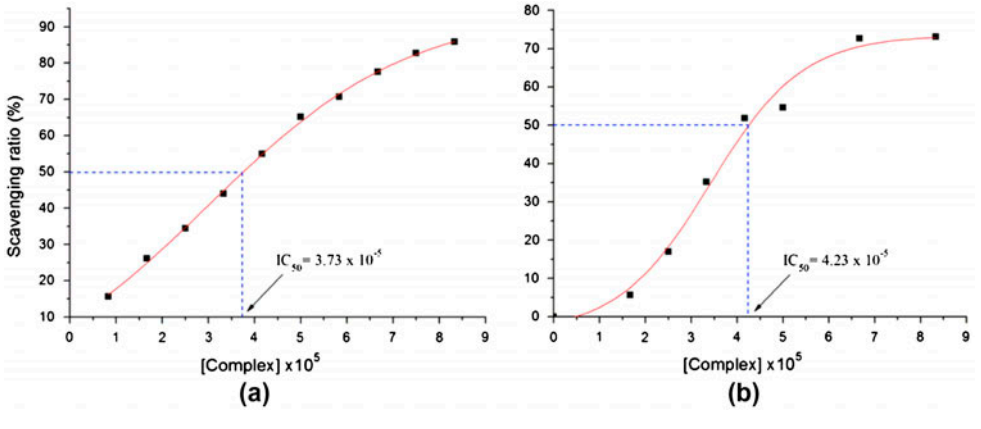

Figure 6. Plots of antioxidation properties for the Y(III) complex. (a) The hydroxyl radical-scavenging effect (%) for the Y(III) complex. (b) The superoxide radical-scavenging effect (%) for the Y(III) complex.

The Y(III) complex shows an IC_{50} value of $4.23 \times 10^{-5}\,M^{-1}$ (figure 6(b)), which indicates that it has potent scavenging activity for superoxide radical (O_2^-). This indicates that the Y(III) complex exhibits good superoxide radical-scavenging activity and may be an inhibitor (or a drug) to scavenge superoxide radical (O_2^-) *in vivo*.

4. Conclusion

A new ligand, bis(*N*-salicylidene)-3-oxapentane-1,5-diamine and its Y(III) complex have been synthesized and characterized. The crystal structure of $Y_2L_2(NO_3)_2{\cdot}2H_2O$ shows eight-coordinate yttrium adopting a distorted square antiprism geometry. The DNA-binding experiments suggest that H_2L and Y(III) complex bind to DNA in a groove mode, and the affinity for DNA is stronger in the case of Y(III) complex when compared with the ligand. The Y(III) complex exhibited potential antioxidant activities against $OH\cdot$ and O_2^- radicals *in vitro*. These findings indicate that Y(III) complex has many potential applications for the development of nucleic acid molecular probes and new therapeutic reagents for diseases at the molecular level, and warrant further *in vivo* experiments and pharmacological assays.

Supplementary material

Crystallographic data (excluding structure factors) for the structure reported in this paper have been deposited with the Cambridge Crystallographic Data Center with reference number CCDC 917806. Copies of the data can be obtained, free of charge, on application to the CCDC, 12 Union Road, Cambridge CB2 1EZ, UK. Tel: +44 01223 762910; Fax: +44 01223 336033; E-mail: deposit@ccdc.cam.ac.uk or http://www.ccdc.cam.ac.uk.

Acknowledgments

The authors acknowledge the financial support and grant from 'Qing Lan' Talent Engineering Funds by Lanzhou Jiaotong University. This work is also supported by the Fundamental Research Funds for the Gansu Province Universities (212086).

References

[1] Y.T. Sun, S.Y. Bi, D.Q. Song, C.Y. Qiao, D. Mu, H.Q. Zhang. *Sens. Actuators, B*, **129**, 799 (2008).
[2] Y. An, Y.Y. Lin, H. Wang, H.Z. Sun, M.L. Tong, L.N. Ji, Z.W. Mao. *Dalton Trans.*, **2007**, 1250 (2007).
[3] C.M. Che, M. Yang, K.H. Wong, H.L. Chan, W. Lam. *Chem. Eur. J.*, **5**, 3350 (1999).
[4] B. Chen, S. Wu, A. Li, F. Liang, X. Zhou, X. Cao, Z. He. *Tetrahedron*, **62**, 5487 (2006).
[5] C.Y. Wei, G.Q. Jia, J.L. Yuan, Z.C. Feng, C. Li. *Biochemistry*, **45**, 6681 (2006).
[6] A.A. Ghazaryan, Y.B. Dalyan, S.G. Haroutiunian, A. Tikhomirova, N. Taulier, J.W. Wells, T.V. Chalikian. *J. Am. Chem. Soc.*, **128**, 1914 (2006).
[7] V. Uma, M. Elango, B.U. Nair. *Eur. J. Inorg. Chem.*, **22**, 3484 (2007).
[8] M. Demeunynck, C. Bailly, W.D. Wilson (Eds). *Small Molecule DNA and RNA Binders,* Wiley-VCH, Weinheim (2003).
[9] R.W.Y. Sun, D.L. Ma, E.L.M. Wong, C.M. Che. *Dalton Trans.*, **2007**, 4884 (2007).
[10] C. Moucheron. *New J. Chem.*, **33**, 235 (2009).
[11] K.E. Erkkila, D.T. Odom, J.K. Barton. *Chem. Rev.*, **99**, 2777 (1999).
[12] L.N. Ji, X.H. Zou, J.G. Lin. *Coord. Chem. Rev.*, **513**, 216 (2001).
[13] B.M. Zeglis, V.C. Pierre, J.K. Barton. *Chem. Commun.*, **44**, 4565 (2007).

[14] M. Tümer, H. Köksal, M.K. Sener, S. Serin. *Transition Met. Chem.*, **24**, 414 (1999).
[15] Z.M. Wang, H.K. Lin, S.R. Zhu, T.F. Liu, Z.F. Zhou, Y.T. Chen. *Anti-Cancer Drug Des.*, **15**, 405 (2000).
[16] F.H. Lia, G.H. Zhao, H.X. Wu, H. Lin, X.X. Wu, S.R. Zhu, H.K. Lin. *J. Inorg. Biochem.*, **100**, 36 (2006).
[17] H.X. Xu, H.Y. Zhang, X.G. Qu. *J. Inorg. Biochem.*, **100**, 1646 (2006).
[18] A. Cha, G.E. Snyder, P.R. Selvin, F. Bezanilla. *Nature*, **402**, 809 (1999).
[19] P. Caravan, J. Ellison, T. McMurry, R. Lauffer. *Chem. Rev.*, **99**, 2293 (1999).
[20] K. Wang, R. Li, Y. Cheng, B. Zhu. *Coord. Chem. Rev.*, **192**, 297 (1999).
[21] M. Marinić, I. Piantanida, G. Rusak, M. Žinić. *J. Inorg. Biochem.*, **100**, 288 (2006).
[22] Z.Y. Yang, B.D. Wang, Y.H. Li. *J. Organomet. Chem.*, **691**, 4156 (2006).
[23] B.D. Wang, Z.Y. Yang, T.R. Li. *Bioorg. Med. Chem.*, **14**, 6012 (2006).
[24] S. Satyanaryana, J.C. Dabrowiak, J.B. Chaires. *Biochemistry*, **32**, 2573 (1993).
[25] J. Marmur. *J. Mol. Biol.*, **3**, 208 (1961).
[26] S.M. Nalson, V. Knox. *J. Chem. Soc., Dalton Trans.*, 2525 (1983).
[27] Bruker, *SMART, SAINT and SADABS*, Bruker AXS Inc., Madison, WI (2000).
[28] G.M. Sheldrick. *SHELXTL*, Siemens Analytical X-ray Instruments, Inc., Madison, WI (1996).
[29] C.P. Tan, J. Liu, L.M. Chen, S. Shi, L.N. Ji. *J. Inorg. Biochem.*, **102**, 1644 (2008).
[30] A.M. Pyle, J.P. Rehmann, R. Meshoyrer, C.V. Kumar, N.J. Turro, J.K. Barton. *J. Am. Chem. Soc.*, **111**, 3051 (1989).
[31] A. Wolf, G.H. Shimer, T. Meehan. *Biochemistry*, **26**, 6392 (1987).
[32] B.C. Baguley, M.L. Bret. *Biochemistry*, **23**, 937 (1984).
[33] J.R. Lakowicz, G. Webber. *Biochemistry*, **12**, 4161 (1973).
[34] C.C. Winterbourn. *Biochem. J.*, **198**, 125 (1981).
[35] C.C. Winterbourn. *Biochem. J.*, **182**, 625 (1979).
[36] Z.Y. Guo, R.E. Xing, S. Liu, H.H. Yu, P.B. Wang, C.P. Li, P.C. Li. *Bioorg. Med. Chem. Lett.*, **15**, 4600 (2005).
[37] C. Beauchamp, I. Fridovich. *Anal. Biochem.*, **44**, 276 (1971).
[38] Q.H. Luo, Q. Lu, A.B. Dai, L.G. Huang. *J. Inorg. Biochem.*, **51**, 655 (1993).
[39] W.K. Dong, G. Wang, S.S. Gong, J.F. Tong, Y.X. Sun, X.H. Gao. *Transition Met. Chem.*, **37**, 271 (2012).
[40] K. Nakamoto, *Infrared and Raman Spectra of Inorganic and Coordination Compounds*, 4th Edn, p. 284, John Wiley & Sons, New York (1986).
[41] L. Casella, M. Gullotti, A. Pintar, L. Messori, A. Rockenbauer, M. Györ. *Inorg. Chem.*, **26**, 1031 (1987).
[42] W.K. Dong, Y.X. Sun, L. Li, S.T. Zhang, L. Wang, X.Y. Dong, X.H. Gao. *J. Coord. Chem.*, **65**, 2332 (2012).
[43] M.J. Manos, M.S. Markoulides, C.D. Malliakas, G.S. Papaefstathiou, N. Chronakis, M.G. Kanatzidis, P.N. Trikalitis, A.J. Tasiopoulos. *Inorg. Chem.*, **50**, 11297 (2011).
[44] D.S. Sigman, A. Mazumder, D.M. Perrin. *Chem. Rev.*, **93**, 2295 (1993).
[45] D. Suh, J.B. Chaires. *Bioorg. Med. Chem.*, **3**, 723 (1995).
[46] R. Palchaudhuri, P.J. Hergenrother. *Curr. Opin. Biotechnol.*, **18**, 497 (2007).
[47] L.S. Lerman. *J. Mol. Biol.*, **3**, 18 (1961).
[48] B.D. Wang, Z.Y. Yang, P. Crewdson, D.Q. Wang. *J. Inorg. Biochem.*, **101**, 1492 (2007).
[49] T.M. Kelly, A.B. Tossi, D.J. McConnell, T.C. Strekas. *Nucleic Acids Res.*, **13**, 6017 (1985).
[50] M.F. Wang, Z.Y. Yang, Z.C. Liu, Y. Li, T.R. Li, M.H. Yan, X.Y. Cheng. *J. Coord. Chem.*, **65**, 3805 (2012).
[51] Y.C. Liu, K.J. Zhang, R.X. Lei, J.N. Liu, T.L. Zhou, Z.Y. Yang. *J. Coord. Chem.*, **65**, 2041 (2012).
[52] P. Kapoor, R.V. Singh, N. Fahmi. *J. Coord. Chem.*, **65**, 262 (2012).
[53] M.F. Wang, Z.Y. Yang, Y. Li, H.G. Li. *J. Coord. Chem.*, **64**, 2974 (2012).
[54] J.H. Huang, X.M. Wang, L.S. Ding. *J. Coord. Chem.*, **64**, 2791 (2012).
[55] J.K. Barton, A.T. Danishefsky, J.M. Goldberg. *J. Am. Chem. Soc.*, **106**, 2172 (1984).
[56] M. Cory, D.D. McKee, J. Kagan, D.W. Henry, J.A. Miller. *J. Am. Chem. Soc.*, **107**, 2528 (1985).
[57] M.J. Waring. *J. Mol. Biol.*, **13**, 269 (1965).
[58] V.G. Vaidyanathan, B.U. Nair. *J. Inorg. Biochem.*, **94**, 121 (2003).
[59] R. Vijayalakshmi, M. Kanthimathi, V. Subramanian, B.U. Nair. *Biochim. Biophys. Acta*, **1475**, 157 (2000).
[60] H.L. Wu, J.K. Yuan, Y. Bai, G.L. Pan, H. Wang, J. Kong, X.Y. Fan, H.M. Liu. *Dalton Trans.*, **2012**, 8829 (2012).
[61] H.L. Wu, J.K. Yuan, Y. Bai, G.L. Pan, H. Wang, X.B. Shu. *J. Photochem. Photobiol., B*, **107**, 65 (2012).
[62] Z.Y. Yang, B.D. Wang, Y.H. Li. *J. Organomet. Chem.*, **691**, 4159 (2006).
[63] J.B. LePecq, C. Paoletti. *J. Mol. Biol.*, **27**, 87 (1967).
[64] Q. Wang, Z.Y. Yang, G.F. Qi, D.D. Qin. *Eur. J. Med. Chem.*, **44**, 2425 (2009).
[65] Z.A. Taha, A.M. Ajlouni, W.A. Momani, A.A. Al-Ghzawi. *Spectrochim. Acta, Part A*, **81**, 570 (2011).
[66] T.R. Li, Z.Y. Yang, B.D. Wang, D.D. Qin. *Eur. J. Med. Chem.*, **43**, 1688 (2008).